Transport and magnetic properties of the $(Eu,Ce)_2(Ba,Eu)_2Cu_3O_{9-\delta}$-type and T^*-type superconductors: Dependence of T_c on the size of the rare-earth ion

S. Ikegawa,* T. Wada,† T. Yamashita,‡ H. Yamauchi, and S. Tanaka
Superconductivity Research Laboratory, International Superconductivity Technology Center, 10-13 Shinonome 1-chome, Koto-ku, Tokyo 135, Japan

(Received 30 August 1991; revised manuscript received 18 November 1991)

The electrical transport properties and magnetic susceptibility of $(L_{2/3}Ce_{1/3})_2(La_{1/3}Ba_{1/3}Sr_{1/3})_2Cu_3O_{9-\delta}$ (2:2:3 phase) where L is a rare-earth element are measured and compared with those of the T^* phase ($Nd_{1.4}Ce_{0.2}Sr_{0.4}Cu_{1-x}Zn_xO_{4-\delta}$ and $La_{1.8-x}L_xSr_{0.2}CuO_{4-\delta}$) in order to investigate why the superconducting transition temperature (T_c) depends on the ionic radius of the atom L. For 2:2:3 samples with L=Eu, Dy, Y, or Ho, the smaller the size of the L^{3+} ion, the lower is the value of T_c, while the Hall coefficient (R_H) remains at the same level at temperatures above 130 K. This is in contrast to the case of $La_{1.8-x}L_xSr_{0.2}CuO_{4-\delta}$ with L=Sm, Eu, or Gd, in which the decrease in T_c with decreasing ionic radius of the L atom may be attributed to the reduction in the carrier concentration. The resistivity, R_H, and Seebeck coefficient for a nonsuperconducting 2:2:3 sample containing small L^{3+} ions are all parallel to those of a nonsuperconducting T^*-phase sample with Zn doping. Judging from these experimental results, we suggest that a "disordered potential" similar to the case of the Zn-doped T^*-phase compound exists in the nonsuperconducting 2:2:3 compound.

I. INTRODUCTION

A variety of superconducting cuprates[1] have been discovered, and their superconducting transition temperatures (T_c) range up to 127 K.[2] Many attempts have been made to extract physical parameters, such as the carrier concentration,[3,4] which are correlated with the magnitude of T_c. Such attempts are indispensable not only to elucidate the mechanism of high-temperature superconductivity, but also to develop other superconducting materials. The Hall coefficient R_H of the superconducting cuprates has attracted much attention of the researchers because of the following reasons. First, it can provide a rough estimation for the mobile-carrier concentration, though it is known that the Hall number n_H [$=(eR_H)^{-1}$] is generally larger than the hole concentration estimated chemically from the oxygen content.[5] The second reason is that the slope of the n_H-versus-temperature curve has been reported to be correlated with the magnitude of T_c.[5,6]

Several families of superconducting cuprates which contain fluorite-type blocks[1] in their crystal structures have been discovered. Sawa *et al.*[7] discovered the $(Eu,Ce)_2(Ba,Eu)_2Cu_3O_9$-type superconductors. Wada *et al.*[8] reported that the magnitude of T_c for $(L_{2/3}Ce_{1/3})_2(La_{1/3}Ba_{1/3}Sr_{1/3})_2Cu_3O_{9-\delta}$ (hereafter, we call the 2:2:3 phase) strongly depended on the ionic radius of the rare-earth element (L) located in the fluorite-type block. This contrasts with the case of $RBa_2Cu_3O_7$ (1:2:3 phase),[9] where the magnitude of T_c depends very weakly on the radius of the R^{3+} ion. The dependence of T_c on the radius of the rare-earth ion in the fluorite block was also observed for other systems: $La_{1.8-x}L_xSr_{0.2}CuO_{4-\delta}$ (T^* phase),[10] $L_{1.85}Ce_{0.15}CuO_{4-\delta}$ (T' phase),[11] $Bi_2Sr_2(L_{1-x}Ce_x)_2Cu_2O_{10+\delta}$ (Bi 2:2:2:2: phase),[12] and $(Pb_{1/2}Cu_{1/2})(Sr_{7/8}L_{1/8})_2(L_{3/4}Ce_{1/4})_2Cu_2O_z$.[13] In some of these systems, the carrier concentration may be different, depending on the compounds containing different kinds of rare-earth elements, and may affect the magnitude of T_c. In other systems, however, T_c changes sharply (down to zero), depending on the radius of the L^{3+} ion, while the carrier concentration remains at nearly the same level. The latter case is important for the study of structural chemistry and electronic states which are related to high-temperature superconductivity. This case includes the 2:2:3 compounds with L=Eu, Dy, Y, and Ho (Ref. 8) and the Bi 2:2:2:2 compounds with L=Nd, Sm, Eu, Gd, and Dy.[12]

In the present work, we investigated the effects of the rare-earth ion on the normal-state transport properties, i.e., resistivity R_H and Seebeck coefficient, of the 2:2:3 phase. Previously, we reported preliminary data on some of these properties.[14,15] In the 2:2:3 phase, the smaller the size of the L^{3+} ion, the lower was the value of T_c, while R_H remained at the same level at temperatures above 130 K.[14] On the other hand, in the T^* phase, the smaller the size of the L^{3+} ion, the lower were both the carrier concentration and T_c. The transport properties of T^* samples in which Cu ions were partially substituted by Zn ions were compared with those of 2:2:3 samples. Each of the R_H-vs-T curves for all the 2:2:3 and T^* samples possessed a maximum at T_p in the range 90–150 K. In heavy-fermion compounds,[16] an anomalous temperature dependence of R_H, including a peak structure (at T_p) was observed. It was ascribed to skew scattering, and the skew-scattering contribution to R_H at temperatures higher than T_p was proportional to the magnetic susceptibility.[16] Therefore, the relations between the electrical transport and magnetic properties in the normal state were also investigated.

II. EXPERIMENTS

Three sets of the samples were prepared by a conventional solid-state reaction method. Their compositions are listed in Table I with the abbreviations for the sample names. The first set is $(L_{2/3}Ce_{1/3})_2(La_{1/3}Ba_{1/3}Sr_{1/3})_2Cu_3O_{9-\delta}$ with L = Eu, Dy, Y, and Ho (L 2:2:3 series). For the 2:2:3 compounds, the oxygen nonstoichiometry δ can be either positive or negative (between the +0.3 and −0.3) depending on the oxygen pressure in the final heat treatment.[8] In the present work, the samples were prepared by the procedure described elsewhere,[8] and the final heat treatment was made in an O_2 gas at 3 atm. The oxygen contents and lattice constants were previously reported[8] for samples prepared under the same conditions as those employed in the present work.

The second set is $Nd_{1.4}Ce_{0.2}Sr_{0.4}Cu_{1-x}Zn_xO_{4-\delta}$ with x = 0, 0.015, and 0.02 (Zn-doped T^* series), which was prepared by the procedure described elsewhere.[17] The final heat treatment was made at 500° C for 10 h in an O_2 gas at 1 atm. For the same Zn-doped T^* samples, the results of x-ray diffraction were previously reported.[17]

The third set is $La_{1.8-x}L_xSr_{0.2}CuO_{4-\delta}$ with L = Sm (x = 1), Eu (x = 0.9), and Gd (x = 0.9) (L T^* series). These compositions were reported by Cheong *et al.*[10] to be single phase. High-purity powders of La_2O_3, Sm_2O_3, Eu_2O_3, Gd_2O_3, $SrCO_3$, and CuO were used as starting materials. Mixed powders of the desired compositions were calcined at 950–1100° C for a total of 48 h with four intermediate regrindings. The samples were sintered at 1130%°C for 12 h in the air. Finally, the samples were annealed in an O_2 gas at 80 atm. In this treatment the temperature was lowered stepwise: at 850 °C for 0.5 h, 600 °C for 5h, and 400 °C for 5h. The oxygen contents of the L T^* samples were determined using a Coulometric titration technique.[18] In this method, after dissolving the sample and CuCl in 1N HCl, the amount of remaining Cu^+ is determined by Coulometric analysis. This technique can determine the oxygen content with an accuracy similar to or higher than an iodometric titration technique.[3]

The phases present and lattice constants were determined by powder x-ray diffraction (XRD) using Cu-$K\alpha$ radiation. The dc magnetic susceptibility was measured using a superconducting quantum interference device (SQUID) magnetometer (Quantum Design model MPMS). For superconducting properties it was measured with decreasing temperature under an applied field of 1 mT. The superconducting transition temperatures T_c were defined as the onset of diamagnetic signal and are listed in Table I. For the normal-state susceptibility, a field of 0.5 T was applied.

Hall-effect and resistivity measurements were made simultaneously for the samples thinned to 0.2 mm. For the Hall measurements, the maximum applied field was 6 T and the maximum applied current was 50 mA. The details of the measurement conditions were described elsewhere.[17] The Seebeck coefficients were measured by a conventional steady-state technique using two pairs of copper-Constantan thermocouples.[15] The distance and temperature difference between the two thermocouples were, respectively, ~3 mm and less than 0.5 K.

In the following results for each of the L 2:2:3, Zn-doped T^*, and L T^* compounds are presented separately in Sec. III. In Sec. IV a comparison is made of the results for the L 2:2:3, Zn-doped T^*, and L T^* samples.

III. RESULTS

A. $(L_{2/3}Ce_{1/3})_2(La_{1/3}Ba_{1/3}Sr_{1/3})_2Cu_3O_{9-\delta}$

First, we deal with the structural chemistry of the L 2:2:3 series. (See Fig. 1 of Ref. 19 for the crystal structure and atomic sites of the 2:2:3 phase.) According to the XRD data, the sample with L = Eu (Eu 2:2:3) was single phase. For the samples with L = Dy, Y, and Ho, a peak, which was probably due to CeO_2, was seen in the XRD patterns. The ratios of the intensities of this peak to that of the main peak for the 2:2:3 phase were 0.4%, 1.4% and 1.6% for the samples with L = Dy (Dy 2:2:3), Y (Y 2:2:3), and Ho (Ho 2:2:3), respectively. CeO_2 is a nonmagnetic insulator and, therefore, does not significantly affect the low-temperature transport properties. As the size of the L^{3+} ion decreased, both of the lattice constants a and c decreased, while the oxygen content remained constant within an accuracy of ±1.2%.[8] The L^{3+} ions are thought to occupy the site with a coordination number of 8 ($A1$ site in Fig. 1 of Ref. 19), which is included in the fluorite-type block. The rest of the $A1$ site is occupied by Ce^{4+}. The values of the average ionic radius of the cations at the $A1$ site [$r(A1)$] can be obtained using the ionic radii listed in Shannon's table[20] and are given in Table I.

Figure 1 shows the Meissner signals of the 2:2:3 samples. T_c values for Eu 2:2:3 and Dy 2:2:3 are 28.5 and about 7 K, respectively. The diamagnetic signal for Dy 2:2:3 is small, i.e., 5% of a full Meissner signal ($=-1/4\pi$ in cgs units). This signal is superposed on the Curie paramagnetic signal due to Dy^{3+} ions. For Y 2:2:3 and Ho 2:2:3, no superconducting transitions are observed down to 2 K in both susceptibility and resistivity data. The magnitude of T_c decreases as the ionic radius of L^{3+} decreases.

The temperature dependences of the resistivity and Hall coefficients are shown in Fig. 2.[14] The resistivity (ρ) curve for each of the four samples possesses a minimum with respect to temperature in the range 120–180 K. At temperatures above ~150 K, ρ values for the four samples are not much different. At temperatures below the minimum, ρ increases as the size of the L^{3+} ion decreases (from that of Eu^{3+} to that of Ho^{3+}). Each of the four R_H-vs-T curves has a maximum located at T_p around 110–130 K. At temperatures above T_p, R_H values were nearly identical for all the 2:2:3 samples, except for Ho 2:2:3, which has a slightly larger value of R_H than those of the other samples. This result agrees with the oxygen-analysis data.[8] At temperatures below T_p, R_H values for the four samples decrease with decreasing temperature and their slopes (positive) are different for samples containing different kinds of L^{3+} ion. The slope decreases as the size of the L^{3+} ion decreases (from that of Eu^{3+} to

TABLE I. Composition, oxygen pressure at a final heat treatment [$P(O_2)$], superconducting transition temperature (T_c), and average ionic radius of the $A1$ site cations [$r(A1)$] of the samples.

Sample type	Composition	$P(O_2)$ (atm)	T_c (K)	$r(A1)$ (Å)
L 2:2:3 series				
Eu 2:2:3	$(Eu_{2/3}Ce_{1/3})_2(La_{1/3}Ba_{1/3}Sr_{1/3})_2Cu_3O_{9-\delta}$	3	28.5	1.034
Dy 2:2:3	$(Dy_{2/3}Ce_{1/3})_2(La_{1/3}Ba_{1/3}Sr_{1/3})_2Cu_3O_{9-\delta}$	3	7	1.008
Y 2:2:3	$(Y_{2/3}Ce_{1/3})_2(La_{1/3}Ba_{1/3}Sr_{1/3})_2Cu_3O_{9-\delta}$	3	<2	1.003
Ho 2:2:3	$(Ho_{2/3}Ce_{1/3})_2(La_{1/3}Ba_{1/3}Sr_{1/3})_2Cu_3O_{9-\delta}$	3	<2	1.000
Zn-doped T^* series				
0% Zn-doped T^*	$Nd_{1.4}Ce_{0.2}Sr_{0.4}CuO_{4-\delta}$	1	23.1	1.081
1.5% Zn-doped T^*	$Nd_{1.4}Ce_{0.2}Sr_{0.4}Cu_{0.985}Zn_{0.015}O_{4-\delta}$	1	<2	1.081
2% Zn-doped T^*	$Nd_{1.4}Ce_{0.2}Sr_{0.4}Cu_{0.98}Zn_{0.02}O_{4-\delta}$	1	<2	1.081
L T^* series				
Sm T^*	$La_{0.8}SmSr_{0.2}CuO_{4-\delta}$	80	21	1.079
Eu T^*	$La_{0.9}Eu_{0.9}Sr_{0.2}CuO_{4-\delta}$	80	12	1.075
Gd T^*	$La_{0.9}Gd_{0.9}Sr_{0.2}CuO_{4-\delta}$	80	<2	1.064

that of Ho^{3+}). Thus the slope is suspected to be strongly correlated to the magnitude of T_c. The R_H data given in Fig. 2 were measured using an applied magnetic field of 6 T. For each of the four samples, the dependence of the Hall coefficient on magnetic field was investigated at two temperatures below and above T_p, i.e., 50 and 210 K. No field dependences are observed, as shown in Fig. 3 (for Eu 2:2:3 and Y 2:2:3 samples). The data for fields below 3 T are relatively scattered because of small Hall voltages.

The Seebeck coefficient S is plotted in Fig. 4 for the superconducting 2:2:3 (Eu 2:2:3) and nonsuperconducting 2:2:3 (Y 2:2:3) samples.[15] The S-vs-T curve for Eu 2:2:3 has a peak (at T_q) around 170 K. Throughout the measured temperature range, S for Y 2:2:3 is larger than that for Eu 2:2:3. T_q for Y 2:2:3 is 190 K, which is slightly higher than that for Eu 2:2:3.

The L^{3+} ions contained in each sample have different magnetic moments. The normal-state magnetic susceptibility (χ) was measured to investigate the relation between the transport and magnetic properties. Figure 5 shows the results for the four samples. No correlations were recognized between the behavior of the R_H-vs-T curves [Fig. 2(b)] and the χ-vs-T curves (Fig. 5). The inverse susceptibility data for the samples except for the Eu 2:2:3 sample are plotted against temperature in Fig. 6. The curves for Dy 2:2:3 and Ho 2:2:3 obeys the Curie-Weiss law $\chi = C/(T-\Theta)$. The effective Bohr magnetons per L^{3+} ion calculated from the Curie constant are $10.3\mu_B$ for both Dy 2:2:3 and Ho 2:2:3. They are in good agreement with the values for χ and Ho^{3+}, i.e., $10.6\mu_B$ for both ions. The Weiss temperatures (Θ) are -6.8 and

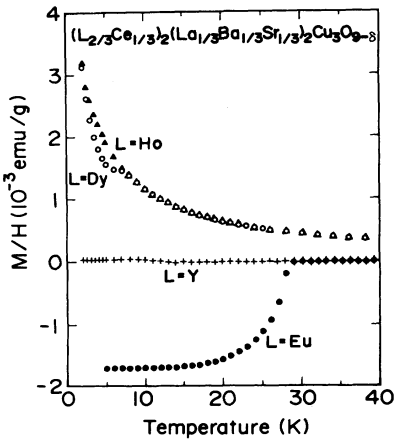

FIG. 1. Superconducting diamagnetic susceptibility (Meissner effect) for $(L_{2/3}Ce_{1/3})_2(La_{1/3}Ba_{1/3}Sr_{1/3})_2Cu_3O_{9-\delta}$ with L = Eu, Dy, Y, and Ho, measured in an applied field of 1 mT.

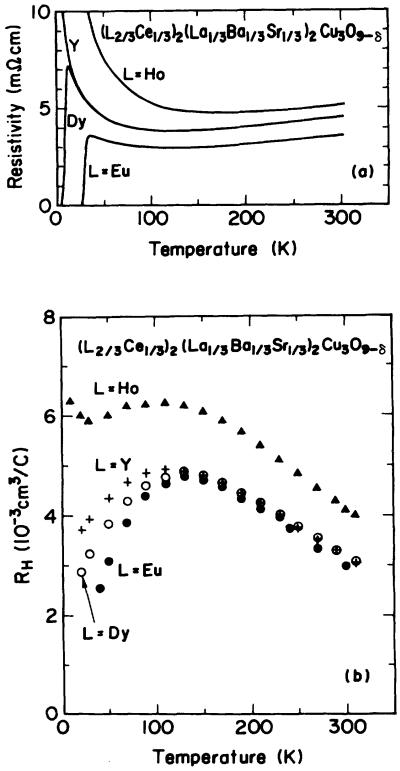

FIG. 2. Temperature dependence of (a) resistivity and (b) Hall coefficients for $(L_{2/3}Ce_{1/3})_2(La_{1/3}Ba_{1/3}Sr_{1/3})_2Cu_3O_{9-\delta}$ with L = Eu, Dy, Y, and Ho.

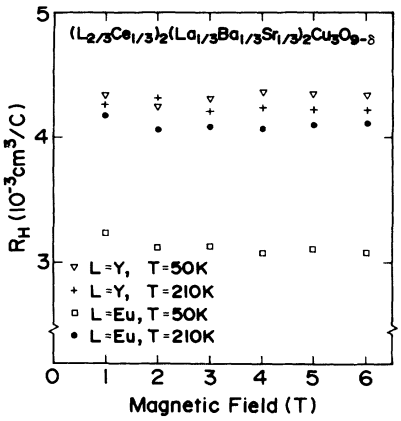

FIG. 3. Field dependence of Hall coefficients at 50 and 210 K for $(Eu_{2/3}Ce_{1/3})_2(La_{1/3}Ba_{1/3}Sr_{1/3})_2Cu_3O_{9-\delta}$ and $(Y_{2/3}Ce_{1/3})_2(La_{1/3}Ba_{1/3}Sr_{1/3})_2Cu_3O_{9-\delta}$.

-10.0 K for Dy 2:2:3 and Ho 2:2:3, respectively. This implies an antiferromagnetic correlations between the L^{3+} ions.

The temperature dependence of the magnetic susceptibility of Eu 2:2:3 per mole of Eu is shown in Fig. 7. The ground state of the Eu^{3+} ion is $J=0$, but one has to account for the contribution from the excited levels ($J\neq 0$), which are thermally populated at high temperatures because the J multiplet intervals are comparable to k_BT. The formula derived by Van Vleck [Eq. (16) in Ref. 21] was used to fit the susceptibility data as was done for Eu_2CuO_4 by Tovar *et al.*[22] and Seaman *et al.*[23] As the fitting parameter, a spin-orbit coupling constant A which determines the J multiplet intervals, was employed. The solid line in Fig. 7 is the fitted curve with $A=438\pm4$ K. This value for A is in good agreement with that ($\sim$440 K) obtained for Eu_2CuO_4.[22] Therefore, most of the Ce ions contained in the Eu 2:2:3 samples are considered to be nonmagnetic. According to Van Vleck's formula, the susceptibility is expected to level off at temperatures below 100 K. However, the experimentally obtained susceptibility for Eu 2:2:3 increases further as the temperature decreases. For Y 2:2:3 it was observed that the susceptibility increases with decreasing temperature, as shown in Fig. 6, in spite of the fact that an Y^{3+} ion does not carry localized magnetic moments.

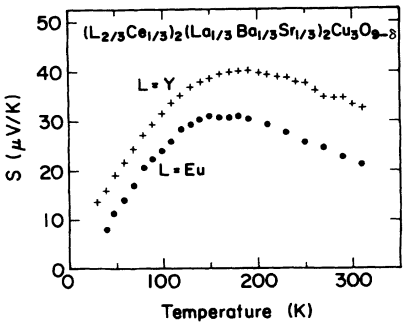

FIG. 4. Temperature dependence of Seebeck coefficients for $(Eu_{2/3}Ce_{1/3})_2(La_{1/3}Ba_{1/3}Sr_{1/3})_3Cu_3O_{9-\delta}$ and $(Y_{2/3}Ce_{1/3})_2(La_{1/3}Ba_{1/3}Sr_{1/3})_2Cu_3O_{9-\delta}$.

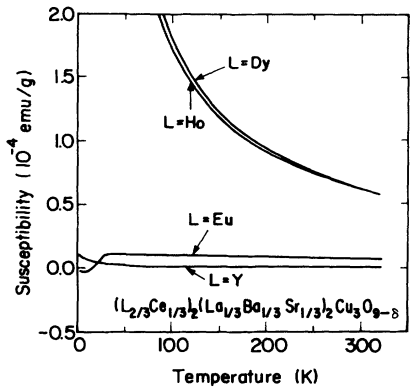

FIG. 5. Temperature dependence of the magnetic susceptibility for $(L_{1/3}Ce_{1/3})_2(La_{1/3}Ba_{1/3}Sr_{1/3})_2Cu_3O_{9-\delta}$ with L=Eu, Dy, Y, and Ho, measured in an applied field of 0.5 T.

B. $Nd_{1.4}Ce_{0.2}Sr_{0.4}Cu_{1-x}Zn_xO_{4-\delta}$

In the series of samples $Nd_{1.4}Ce_{0.2}Sr_{0.4}CuO_{4-\delta}$ doped with Zn (Zn-doped T^* series), the temperature dependence of R_H was found to be similar to the case of the L 2:2:3 series. In the following, the Zn-doped T^* series are compared with the L 2:2:3 series in terms of the transport properties. The samples with $x=0$ and 0.015 are confirmed to be single phase by XRD. The sample with $x=0.02$ contained about 7% T' phase as an impurity phase. Probably, the impurity phase in the sample is an insulator or semiconductor and has little influence on R_H. The superconducting properties of these samples were previously reported.[17] As the Zn content x increased, T_c decreased monotonically. When x reached the value of 0.015, superconductivity disappeared.

The resistivity and Hall-coefficient data for the Zn-doped T^* samples are shown in Fig. 8. Each of the ρ-vs-T curves has a minimum at a temperature in the range 110–180 K. The resistivity increases with increasing Zn content, especially at temperatures below 150 K. Each of the R_H-vs-T curves has a maximum at T_p in the range 110–150 K. R_H for 1.5% Zn-doped T^* at temperatures higher than 150 K is nearly the same as that for 0% Zn-doped T^*. At temperatures lower than T_p, the slope of the R_H-vs-T curve is positive and decreases with increasing Zn context. The slope below T_p appears to be strong-

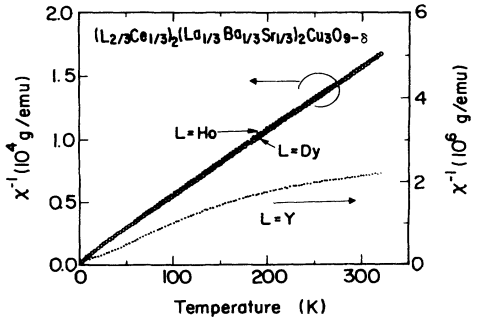

FIG. 6. Temperature dependence of the inverse susceptibility for $(L_{2/3}Ce_{1/3})_2(La_{1/3}Ba_{1/3}Sr_{1/3})_2Cu_3O_{9-\delta}$ with Dy, Y, and Ho.

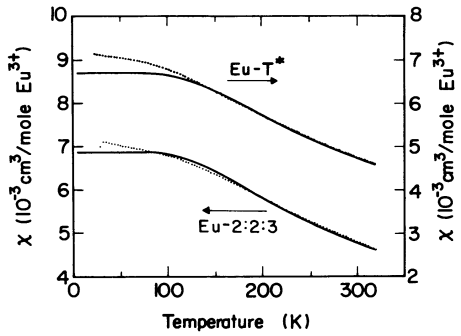

FIG. 7. Temperature dependence of the magnetic susceptibility for $(Eu_{2/3}Ce_{1/3})_2(La_{1/3}Ba_{1/3}Sr_{1/3})_2Cu_3O_{9-\delta}$ (Eu 2:2:3) and $La_{0.9}Eu_{0.9}Sr_{0.2}CuO_{4-\delta}$ (Eu T^*), measured in an applied field of 0.5 T.

ly correlated to the magnitude of T_c, as previously mentioned for the 2:2:3 phase. This behavior is rather contrary to that reported[5,6] for the T, 1:2:3, and Bi 2:2:1:2 phases, for which the slope of R_H-vs-T curve was usually negative and the absolute value of the slope decreased as the magnitude of T_c decreased. It should be noted that an abrupt upturn of R_H with decreasing T was observed for 2% Zn-doped T^* at $T<40$ K, where ρ was larger than 15 m Ω cm and rapidly increased with decreasing T. A similar upturn of R_H was observed for Ho 2:2:3 below 30 K [Fig. 2 (b)], where ρ exceeded 11mΩ cm.

The temperature dependence of Seebeck coefficient is shown in Fig. 9.[15] The S-vs-T curve for 0% (Zn)-doped T^* shows a maximum at $T_q=160$ K. Throughout the measured temperature range, the magnitude of S increases with Zn substitution for Cu. The Zn doping also makes T_q shift from 160 to 210K. The S-vs-T curve for 0% Zn-doped T^* (with $T_c=23.1$ K) is nearly identical to that for Eu-2:2:3 ($T_c=28.5$ K) in Fig. 4. The S-vs-T curve for 1.5% Zn-doped T^* ($T_c<2$ K) is similar to that for Y 2:2:3 ($T_c<2K$) in Fig. 4. For each of Zn-doped T^* and L 2:2:3 phases, the difference in S between the nonsuperconducting and superconducting samples (ΔS) is plotted with respect to temperature in Fig. 10.[15] The temperature dependence of ΔS for the 2:2:3 samples is similar to that for the T^* samples. At low temperatures below 130 K, ΔS is independent of temperature. At temperatures between 130 and 260 K, ΔS increases with increasing temperature. At temperatures above 260 K, ΔS seems to be constant with respect to temperature, although the data points are rather scattered because of the instrumental limitation in temperature control.

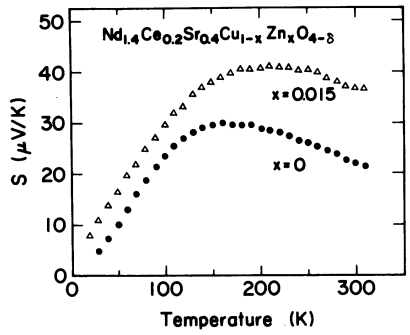

FIG. 9. Temperature dependence of Seebeck coefficients for $Nd_{1.4}Ce_{0.2}Sr_{0.4}Cu_{1-x}Zn_xO_{4-\delta}$.

C. $La_{1.8-x}L_xSr_{0.2}CuO_{4-\delta}$

It was reported that, in the T^* phase, T_c depended on the species of the rare-earth element (L).[10] We investigated three samples with different L's (L T^* series) for the study of the relationship between the ionic radius of L^{3+} and the hole concentration. From the XRD measurements, the samples with $L=$Eu (Eu T^*) and $L=$Gd (Gd T^*) were found to be a single phase of the T^* phase.

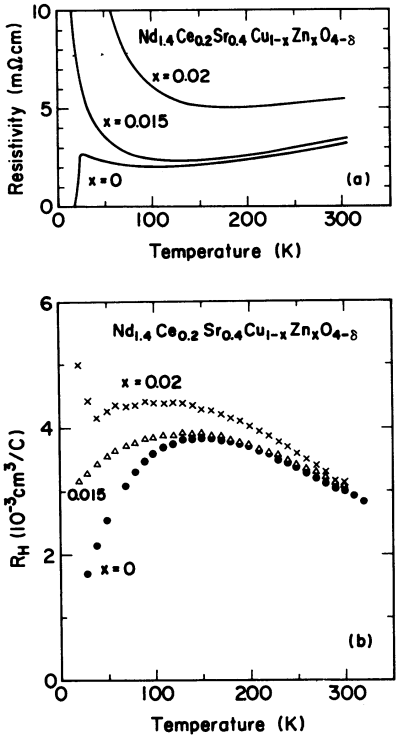

FIG. 8. Temperature dependence of (a) resistivity and (b) Hall coefficients for $Nd_{1.4}Ce_{0.2}Sr_{0.4}Cu_{1-x}Zn_xO_{4-\delta}$.

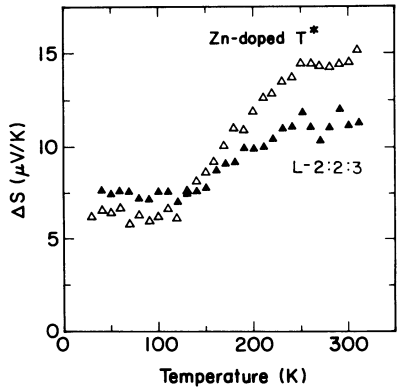

FIG. 10. Difference in Seeback coefficients (ΔS) between the nonsuperconducting and superconducting samples with respect to temperature. The solid and open triangles indicate the cases of the 2:2:3 phase and Zn doping in the T^* phase, respectively.

Unfortunately, it was found that the sample with $L=$Sm included the T' phase as an impurity phase up to an amount of 8–10 %. This impurity phase (T') is probably an insulator or semiconductor and has little influence on R_H. The lattice constants determined by XRD measurements are as follows: $a=3.876$ Å and $c=12.600$ Å for Sm T^*, $a=3.869$ Å and $c=12.580$ Å for Eu T^*, and $a=3.865$ Å and $c=12.567$ Å for Gd T^*. The lengths of both the a and c axes decreased with decreasing the ionic radius of L^{3+}. Sm^{3+}, Eu^{3+}, and Gd^{3+} ions were found to occupy the sites with a coordination number of 8 ($A1$ site) in the fluorite block.[24] The rest of the $A1$ site was occupied by La^{3+} for the case of Eu T^* and Gd T^* (where x in $La_{1.8-x}L_xSr_{0.2}CuO_{4-\delta}$ is 0.9; see Table I).[24] The average ionic radii of the cations at the $A1$ site were calculated using Shannon's table[20] and are listed in Table I.

The Meissner signals of three samples are shown with respect to temperature in Fig. 11. T_c values for Sm T^* and Eu T^* are obtained to be 21 and 12 K. The superconducting transition is not observed for Gd T^* down to 2 K. The magnitude of T_c decreases as the ionic radius of the L^{3+} ion decreases.

The magnitude of Hall coefficient increases as the ionic radius of the L^{3+} ion decreases, as shown in Fig. 12. A similar result for the room-temperature Hall coefficient was recently reported.[25] This suggests that the mobile-carrier concentration decreases as the ionic radius of the L^{3+} ion decreases. The hole concentration p per $[CuO]^{+p}$ unit was also determined chemically by a Coulometric titration technique.[18] The values of p for Sm T^*, Eu T^*, and Gd T^* were 0.133±0.015, 0.106±0.010, and 0.076±0.005, respectively. The error in p for Sm T^* was relatively large because of the impurity phase. The value of p decreases as the ionic radius of the L^{3+} ion decreases since oxygen deficiency increases as the ionic radius of the L^{3+} ion decreases. Assuming a single-band model, Hall coefficients (R_H^c) were estimated using the chemically determined values for p and the relation $R_H^c=V/pe$, where V is half the unit-cell volume. These values are plotted on the right-hand side of Fig. 12. The maximum value of R_H for each of the three samples is identical to or smaller than R_H^c. Similar relations between R_H and p were often observed in superconducting cuprates.[5]

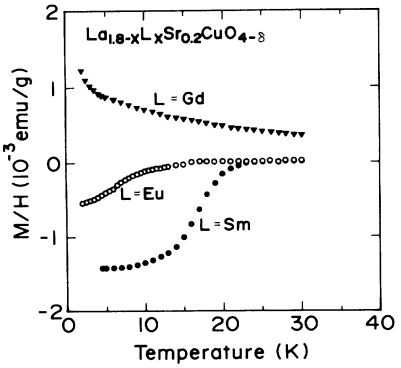

FIG. 11. Superconducting diamagnetic susceptibility (Meissner effect) for $La_{1.8-x}L_xSr_{0.2}CuO_{4-\delta}$ with $L=$Sm ($x=1$), Eu ($x=0.9$), and Gd ($x=0.9$), measured in an applied field of 1 mT.

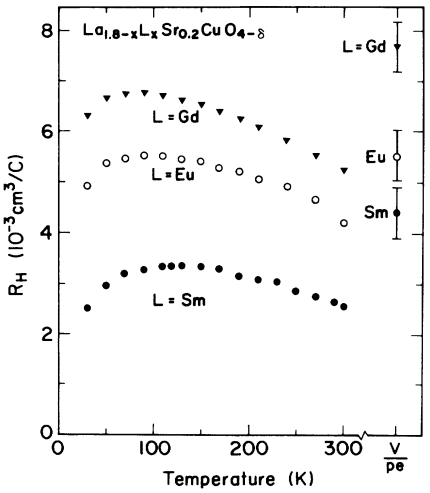

FIG. 12. Temperature dependence of Hall coefficients for $La_{1.8-x}L_xSr_{0.2}CuO_{4-\delta}$ with $L=$Sm ($x=1$), Eu ($x=0.9$), and Gd ($x=0.9$). The estimated values for Hall coefficient (R_H^c) using the chemically determined hole concentration (p) and the relation $R_H^c=V/pe$ (V is half the unit-cell volume) are also plotted on the right-hand side.

The R_H-vs-T curves for Sm T^*, Eu T^*, and Gd T^* have peaks at 120, 100, and 90 K, respectively. The peak temperature T_p appears to be lowered as the chemical doping level is lowered. Similar behavior of T_p was observed for the $(Nd_{0.8-y}Ce_ySr_{0.2})_2CuO_{4-\delta}$ system (T^* phase).[26] For the sample with y in the range 0.09–0.11, the value of p was ~0.14 (Ref. 27) and T_p was ~150 K.[26] For the sample having a smaller value of p of ~0.08 ($y=0.15$),[27] T_p was ~120 K.[26]

The normal-state magnetic susceptibility is shown in Fig. 7 (Eu T^*) and Fig. 13 (Sm T^* and Gd T^*). For Eu T^* the same formula as for Eu 2:2:3 was applied. The solid line in Fig. 7 represents the fitting curve at temperatures above 100 K. This curve is for the value of the spin-orbit coupling constant A, equal to 448±5 K. This value is in good agreement with that obtained for Eu_2CuO_4.[22] Below 100 K, the susceptibility slightly increases with decreasing temperature, contrary to Van

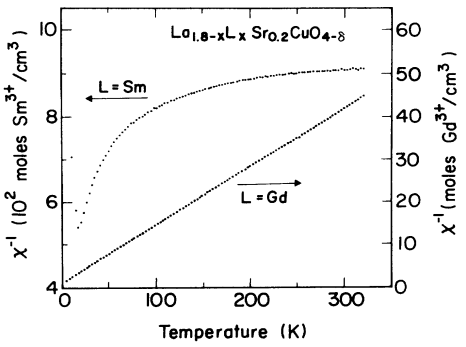

FIG. 13. Temperature dependence of the inverse susceptibility for $La_{0.8}SmSr_{0.2}CuO_{4-\delta}$ and $La_{0.9}Gd_{0.9}Sr_{0.2}CuO_{4-\delta}$.

Vleck's formula. The susceptibility for Gd T^* can be described by the Curie-Weiss law, as shown in Fig. 13. The effective Bohr magneton per Gd^{3+} ion is $7.7\mu_B$, which is in good agreement with the corresponding free-ion value of $7.9\mu_B$. The Weiss temperature Θ is -8.3 K. This suggests an antiferromagnetic correlation between Gd^{3+} ions. For Sm T^* the magnetic susceptibility per mole of Sm (Fig. 13) is similar to that of Sm_2CuO_4.[23] However, the expected susceptibility from a free Sm^{3+} ion calculated using Van Vleck's formula [Eq. (23) in Ref. 21] is larger than the measured value (by a factor of ~ 2 at 50 K). Such a discrepancy might arise from the mixed-valence state of the Sm ion[28] or a certain kind of interaction between the magnetic moment of Sm and the charge carrier.[29] The normal-state magnetic susceptibility data for the L T^* samples (Figs. 7 and 13) do not exhibit clear correlations with the Hall-coefficient data (Fig. 12).

Both the Hall measurement and chemical analysis showed that the hole concentration in the L T^* samples decreases as the ionic radius of the L^{3+} ion decreases. The relation between p and T_c for the L T^* sample series is parallel to that for the $La_{2-x}Sr_xCuO_{4-\delta}$ system reported by Torrance *et al.*[3] The reduction in T_c with decreasing the radius of the L^{3+} ion from that of Sm^{3+} to that of Gd^{3+} is probably caused by the reduction in hole concentration.

IV. DISCUSSION

A. Temperature dependence of the transport coefficient

We discuss the temperature dependence of R_H, S, and ρ for the 2:2:3 and T^* compounds, and it is compared with the theoretical prediction based on a t-J model. Each of the R_H-vs-T curves for the L 2:2:3 samples [Fig. 2(b)] and Zn-doped T^* samples [Fig. 8(b)] commonly possesses a maximum at T_p in the range 110–150 K. The value of the hole concentration p for $Nd_{1.4}Ce_{0.2}Sr_{0.4}CuO_{4-\delta}$ (T^* phase) was reported to be about 0.14.[27] The room-temperature Hall coefficients for all the Zn-doped T^* samples are nearly identical, and therefore, p values for all the Zn-doped T^* samples are considered to be about 0.14. The sheet hole concentration p_{sh} (Ref. 4) for all the L 2:2:3 samples is roughly estimated to be 0.13 from the minimum value of n_H. As the value of p is lowered, T_p is lowered, as shown in Fig. 12. The normal-state magnetic susceptibility for L 2:2:3 and L-T^*, except for Y 2:2:3 and Sm T^*, is considered to be mainly from the moment of the free L^{3+} ions. The temperature dependence of R_H may not be correlated with that of the magnetic susceptibility data. Therefore, the anomalous temperature dependence of R_H cannot be attributed to skew scattering by $4f$ moments. The maximum in the R_H-vs-T curve was observed commonly in the 2:2:3, T^*, and T' compounds.[14] Previously, we ascribed such a maximum to the modification of electronic states in the CuO_2 plane due to an interaction with the neighboring fluorite block.[14] However, Tamegai and Iye[30] recently found that the R_H-vs-T curves for $Nd_{1+x}Ba_{2-x}Cu_3O_{7+\delta}$ with $x=0.2$–0.3 (1:2:3 phase) and $YBa_2(Cu_{0.95}Co_{0.05})_3O_{7+\delta}$ (1:2:3 phase) had maxima around 120 K, which were similar to those for the 2:2:3 phase.[31,14] They claimed that a maximum in R_H was accompanied by an upturn of the resistivity and that this behavior was a universal transport anomaly of the CuO_2 planes when the value of p was in the range 0.1–0.15. In the present work, p values for L 2:2:3 and Zn-doped T^* samples were considered to fall within this range.

The anomalies in R_H and ρ for the 2:2:3 and T^* phases may be related to structural instability, as was pointed out for the 1:2:3 phase.[30] From a neutron-diffraction study for the T^* phase,[32] O(2) atoms (apexes of the CuO_5 pyramids) are believed to be statically disordered about the ideal positions. Bordet *et al.*[33] found that, in $La_{1.13}Tb_{0.81}Pb_{0.06}CuO_{4-\delta}$ (T^* phase), a tetragonal-orthorhombic transition occurred in the temperature range 470–150 K. The low-temperature orthorhombic structure was ascribed to the "ordered canting" of the CuO_5 pyramids and the "corrugation" of the CuO_2 planes, which generated two inequivalent Cu sites in the CuO_2 plane, and the high-temperature tetragonal structure was ascribed to a dynamically disordered canting of the CuO_5 pyramids.[33] Bordet *et al.* observed a similar superstructure for $LaSm_{0.8}Sr_{0.2}CuO_4$ (T^* phase) at 77 K, though the ordering appeared to be short range.[33] Also, for the 2:2:3 phase, a neutron-diffraction study at room temperature revealed that the O(2) atoms (apexes of the CuO_5 pyramids) and Cu(1) atoms are displaced locally from their ideal positions.[34] Therefore, the structural instability associated with the canting of the CuO_5 pyramids is likely to be inherent to the crystal structure of both 2:2:3 and T^* phases and affect the transport properties of the phases. Thus a structural transition or a freezing of dynamically disordered canting may cause anomalies in R_H and ρ at $T\sim 150$ K. In the samples of $Nd_{1.2}Ba_{1.8}Cu_3O_{7+\delta}$ and $YBa_2(Cu_{0.95}Co_{0.05})_3O_{7+\delta}$ in which the maxima in R_H-vs-T curves were reported,[30] disorder can also be introduced into the Ba or the Cu(1) site, as well as into the apex oxygen site. Detailed structural analyses by low-temperature neutron diffraction are required to understand the structural instability at low temperatures.

Tamegai and Iye[30] pointed out that the decrease in R_H and the increase in ρ with decreasing T below 120 K can be explained by gap formation in a hole band, which was postulated to coexist with an electron band (two-band model). According to the present experimental data (given in Figs. 2 and 8), as the temperature approaches zero, the more rapidly ρ increases, the less rapidly the corresponding R_H decreases. This feature seems to be difficult to explain straightforwardly by the gap-formation model. In Sec. IV B we present an explanation from the viewpoint of Anderson localization[35] as well as the Coulomb interaction in the presence of a random potential.[35]

On the basis of a t-J model, Nagaosa and Lee[36] calculated transport coefficients in the uniform resonating-valence-bond (RVB) state in which fermions and spinless bosons are coupled by a gauge field. They obtained $R_H=(R_H^F\chi_B+R_H^B\chi_F)/(\chi_B+\chi_F)$, where χ_F (or χ_B) is the

Landau diamagnetic susceptibility of the fermions (or bosons) and R_H^F (or R_H^B) is the Hall coefficient for the fermions (or bosons). At temperatures above the Bose-Einstein condensation temperature T_{BE}, R_H is governed by the bosons. For this range of temperature, two recent works[37,38] theoretically predicted that R_H increases with decreasing T. For temperatures below T_{BE}, χ_B becomes infinite and $R_H \sim R_H^F = -(1-p)^{-1}$. If $T_{BE} > T_c$, R_H-vs-T curves have maxima at T_{BE}. This can be an alternative explanation of the peak structure of the R_H-vs-T curves. In this case, ρ, calculated by the model, consists mainly of the contribution from the fermions (ρ_F) at temperatures below T_{BE}. The magnitude of ρ_F might increase with decreasing temperature in the range of $T < T_{BE}$ by Anderson localization, which would be suppressed by the gauge field at $T > T_{BE}$.[39]

For most of the superconducting cuprates, the temperature dependence of the Seebeck coefficient (S) shows a maximum at a characteristic temperature in the range 100–200 K and decreases with increasing temperature, even at room temperature where phonon drag is usually less likely.[40] Recently, Kaiser and Mountjoy[41] proposed that this characteristic for S may be explained by a strong electron-phonon coupling, instead of the appearance of the phonon-drag peaks, which disappear as the phonon and electron mean free paths are reduced by increasing the scattering. On the other hand, using a gauge-field theory for a uniform RVB state, Nagaosa and Lee[36] (NL) proposed the relation that $S = S_F + S_B$ (NL model), where the S_F and S_B were the Seebeck coefficient of fermions and bosons and, respectively, estimated using conventional Fermi and Maxwellian statistics for the two-dimensional system. Curve fitting for the data given in Figs. 4 and 9 has previously been made on the basis of the NL model.[15] In doing so, an additional parameter was introduced into the expression for S_B, so that reasonably fitted curves were obtained. At present, whether the strong electron-phonon coupling model or NL model is more plausible is undecided.

The resistivity curves in Figs. 2(a) and 8(a) show minima. In the temperature range where ρ is lower than 10 m Ω cm, the present data for the temperature dependence of ρ are found to be curve fitted by the formula $\rho = a + bT - c\ln T$. In the temperature range where ρ exceeds 10 mΩ cm, the increase in ρ with decreasing T down to 1.6 K (instrumental limit) is steeper than the $-\ln T$ curve and milder than the $\exp(1/T)$ curve of a thermal activation type. Then we plot $\ln\rho$ with respect to $T^{-1/3}$ in Figs. 14 and 15 for, respectively, the samples of the L 2:2:3 and Zn-doped T^* series. Figures 14 and 15 indicate that variable-range hoppings (VRH's) of carriers are probably responsible for the electronic conduction in the range of $\rho \geq 10$ mΩ cm, as often observed in layered cuprates.[42,43] It is not clear whether it is a two-dimensional VRH [$\rho \propto \exp(T^{-1/3})$] or a three-dimensional VRH [$\rho \propto \exp(T^{-1/4})$]. Thus each of the ρ-vs-T curves can be divided into the following three regions as the temperature decreases. In the temperature range from room temperature to the temperature T_r, where resistivity has a minimum (region I), the slope of the ρ-vs-T curve is positive. In the temperature range from T_r to temperatures where $\rho < 10$ mΩ cm (region II), ρ exhibits a logarithmic increase with decreasing temperature. The temperature range (region III) where ρ exceeds 10 mΩ cm, if it exists, is for probable VRH conduction. For $La_{1.85}Sr_{0.15}(Cu_{1-x}Ga_x)O_4$ (Ref. 44) and $Nd_{2-x}Ce_xCuO_4$,[45] as temperature decreased, the minimum in ρ was followed by a logarithmic increase. This was interpreted as the Kondo effect.[44,45] For the present results in region II, however, a weak-localization effect, which is caused by quantum interference of the conduction electrons at the defects,[46] and/or effects of Coulomb interaction between electrons in a random potential[35] in the two-dimensional system are more plausible than the Kondo effect, since at the low-temperature side of region II a VRH conduction region (region III) exists.

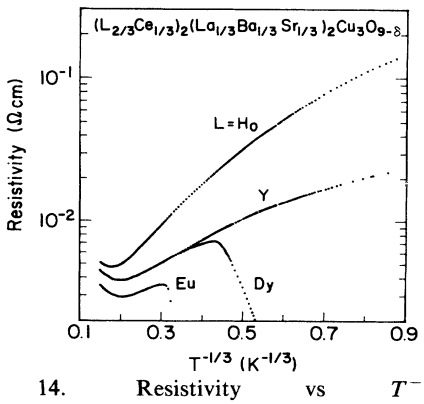

FIG. 14. Resistivity vs $T^{-1/3}$ for $(L_{2/3}Ce_{1/3})_2(La_{1/3}Ba_{1/3}Sr_{1/3})_3Cu_3O_{9-\delta}$ with L = Eu, Dy, Y, and Ho.

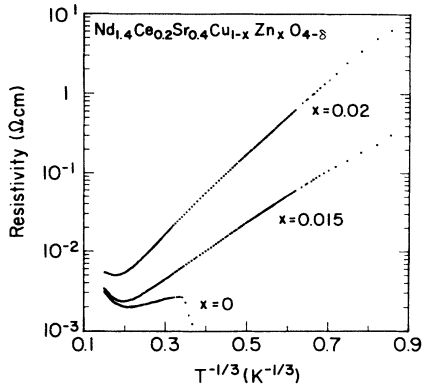

FIG. 15. Resistivity vs $T^{-1/3}$ for $Nd_{1.14}Ce_{0.2}Sr_{0.4}Cu_{1-x}Zn_xO_{4-\delta}$.

B. Compositional dependence of transport properties

We now discuss the effect of rare-earth ions on the normal-state transport properties of the 2:2:3 compounds compared with those of the T^* compounds. Previously (Sec. III B), we have pointed out the similarity of the transport properties of L 2:2:3 to those of Zn-doped T^*. The differences between the superconducting sample (Eu-2:2:3 or 0% Zn-doped T^*) and the nonsuperconducting sample (Y 2:2:3 or 1.5% Zn-doped T^*) are summarized as follows. (1) At temperatures higher than 150 K

(region I), R_H of the nonsuperconducting sample is nearly identical with that of the superconducting one, and also the ρ values of both the samples are not very different. (2) At temperatures in the same range, however, S of the nonsuperconducting sample is larger than that of the superconducting sample. (3) At temperatures lower than 150 K (regions II and III), the nonsuperconducting sample has larger values for S, R_H, and ρ than the superconducting sample.

Because of result (1), result (2) may not be due to the difference in the hole density, but rather due to the difference in the carrier-scattering contribution.[15] The substitution of Zn for Cu in the T^* phase is expected to cause a local destruction of the antiferromagnetic correlations between Cu^{2+} spins[17] and yield a "disordered potential" for carriers in the CuO_2 planes. These effects may bring about an additional carrier scattering and/or a change in the energy dependence of the carrier mean free path and, consequently, an increase in S. In the 2:2:3 phase, a similar disordered potential may be yielded in the CuO_2 planes because of the difference in the radii of the L^{3+} ion. Hereafter the disordered potential is taken to mean a regular potential plus an additional potential with a few percent of randomly distributed defects, such as the substitution of Zn for a few percent of Cu in the CuO_2 plane. It should be noted that, in the case of standard metallic diffusion thermopower, a change in thermopower due to the change in the energy dependence of the carrier mean free path is proportional to temperature. In the present case, however, ΔS (Fig. 10) was not proportional to temperature over a wide temperature range, which might be affected by the complicated temperature dependence of S (Figs. 4 and 9), as mentioned in Sec. IV A.

In the low-temperature range ($T < 150$K), among R_H, S, and ρ, the most striking change was observed for ρ. In the nonsuperconducting sample, ρ strongly increased with decreasing temperature in the range below 50 K, but both R_H and S did not significantly increase in the same range. Therefore, the increase in ρ was not mainly caused by the reduction in the number of mobile carriers. As mentioned in Sec. IV A, the increase in ρ at low temperatures may be ascribed to a weak localization and/or effects of the interaction between electrons in the disordered two-dimensional electronic system in temperature region II and to a VRH conduction in temperature region III. The resistivity data in Figs. 2(a) and 8(a) suggest that the degree of disorder in the potential energy for mobile carriers becomes stronger, as the size of the L^{3+} ion decreases in the L 2:2:3 samples and as the Zn content increases in the Zn-doped T^* samples.

According to theoretical studies for the two-dimensional system,[47] the Hall coefficient is not affected by weak localization. However, a model which took into account both disorder scattering and the electron-electron interaction showed that the resistivity and Hall coefficient exhibited logarithmic increases with decreasing T and the correction term for the Hall coefficient is proportional to that for the resistivity.[48] It is seen from Figs. 2 and 8 that at a fixed temperature, say, 70 K, a sample having a larger resistivity has a larger value for R_H. The latter model can explain this experimental result. Note that in the VRH conduction region (region III), as the temperature decreases, R_H increases for Ho 2:2:3 and 2% Zn-doped T^*. From theoretical analyses for the disordered two-dimensional electronic system,[49,35] Seebeck coefficients are expected to increase logarithmically with decreasing T as is the case with the resistivity, although there has been no experimental verification for this. The data for S in Figs. 4 and 9 show no marked changes below 150 K. Instead, the degree of disorder in the potential energy probably affects the carrier-scattering contribution to S throughout the measured temperature range (20–310 K), as shown in Fig. 10.

One of the possible causes of the disordered potential for carriers is the oxygen vacancy. For the L T^* series, the number of oxygen vacancies increases as the radius of the L^{3+} ion decreases, as mentioned in Sec. III C. In the case of the L 2:2:3 series, the decrease in the radius of the L^{3+} ion can generate such oxygen vacancies in the O(2) (apexes of the CuO_5 pyramids) or O(4) (oxygen in the fluorite-type block) sites which are adjacent to the CuO_2 planes. In this case the total amount of oxygen should remain constant offsetting the oxygen deficiency by introducing oxygen into the O(1) sites. [The O(1) site in the 2:2:3 structure is usually half-filled.[34]] Another possible cause of the disordered potential is a lattice distortion around the fluorite block. In general, a fluorite-type crystal structure can be formed for AX_2, where the ionic-radius ratio $r(A)/r(X)$ is greater than 0.73.[50] If the ratio falls below 0.73, they may adopt the rutile structure where the coordination number of the A ion is 6 instead of 8 of the fluorite-type structure.[50] The average ionic radii of the $A1$ sites (see Table I) of Y 2:2:3 and Ho 2:2:3 are smaller than 73% of the ionic radius of oxygen. As the size of the L^{3+} ion decreases, the lattice distortion around the fluorite block of the 2:2:3 structure may increase. It should be noted that the structural instability associated with the canting of the CuO_5 pyramids (Sec. IV A) also depends on the size of the L^{3+} ion.[33] To confirm such a lattice distortion, detailed structural analysis, e.g., the extended x-ray-absorption fine structure or atomic-pair-distribution analysis of the diffraction data, is required.

From a viewpoint of magnetism in the CuO_2 planes, Yoshida *et al.*[51] recently examined Raman-scattering spectra for $(Eu,Ce)_2(Ba,Eu)_2Cu_3O_{9-\delta}$, which became a superconductor after oxidization, and $(Er, Ce)_2(Ba,La)_2Cu_3O_{9-\delta}$, which did not turn into a superconductor. It was found that no significant changes occurred in two-magnon scattering, even if the ionic radii of the two L^{3+} ions were different.[51] When Cu in $La_{1.85}Sr_{0.15}CuO_{4-\delta}$ was partially substituted by Zn, the Curie-Weiss component was superposed on the normal-state magnetic susceptibility since the antiferromagnetic correlation between Cu^{2+} spins was locally destroyed.[17] In other words, the isolated Cu^{2+} spins were induced around the defects. As for the magnetic susceptibility for Eu 2:2:3, Y 2:2:3, and Eu T^*, it was observed that the unknown component superposed on the contribution from the L^{3+} ion and the unknown component increased with decreasing temperature (see Figs. 6 and 7). If $1.9\mu_B$ is as-

sumed for the isolated spin of Cu^{2+}, the unknown component should, respectively, count (at 50 K) for ~1%, ~7%, and ~2% of Cu for the Eu 2:2:3, Y 2:2:3, and Eu T^* samples. These values are comparable to the case of $La_{1.85}Sr_{0.15}Cu_{1-x}Zn_xO_{4-\delta}$ with $x=0.01-0.04$.[17] The unknown component for Y 2:2:3 is larger than that for Eu 2:2:3. Thus this component may have been caused by isolated Cu^{2+} spins induced by lattice distortion or defects.

Thus, in the L 2:2:3 samples, the compositional dependence of ρ, S, and R_H may suggest that the degree of disorder in the potential energy increases as the size of the L^{3+} ion decreases. This is considered to be one of the reasons why T_c depends on the size of the L^{3+} ion. It is known for conventional BCS superconductors that T_c is reduced as the degree of disorder increases, since the Coulomb repulsive interaction is enhanced in disordered systems.[52] To elucidate the weak-localization effect, magnetoresistance measurements using single crystals are required.

V. SUMMARY

The temperature dependences of ρ, R_H, and S were measured for three series of samples, $(L_{2/3}Ce_{1/3})_2(La_{1/3}Ba_{1/3}Sr_{1/3})_2Cu_3O_{9-\delta}$ (L=Eu, Dy, Y, and Ho), $Nd_{1.4}Ce_{0.2}Sr_{0.4}Cu_{1-x}Zn_xO_{4-\delta}$ ($x=0-0.02$), and $La_{1.8-x}L_xSr_{0.2}CuO_{4-\delta}$ (L=Sm, Eu, and Gd), in order to investigate the dependence of T_c on the ionic radius of the L atom. The magnetic susceptibility in the normal state was also measured. The susceptibility was found to have the main contribution from free L^{3+} ions and no correlations to the magnitude of T_c and also to the R_H-vs-T curve. In the L 2:2:3 series, T_c decreases as the size of the L^{3+} ion decreases (from the size of Eu^{3+} to that of Ho^{3+}), while the hole concentration remains the same. In the L T^* series, the reduction in T_c with decreasing the size of the L^{3+} ion (from the size of Sm^{3+} to that of Gd^{3+}) may be explained by the reduction in the carrier concentration. Each of the R_H-vs-T curves for the 2:2:3 and T^* phases had a maximum at T_p in the range 90–150 K. It was found that the slope of a R_H-vs-T curve below T_p was dependent on the magnitude of T_c. The data of ρ, R_H, and S for the nonsuperconducting 2:2:3 sample containing small L^{3+} ions were all parallel to those of the nonsuperconducting Zn-doped T^* sample. With decreasing temperature below 150 K, ρ for both samples showed a logarithmic increase followed by variable-range-hopping conduction. Throughout the measured temperature range, S's for both nonsuperconducting samples were larger than those of the superconducting samples. Therefore, a "disordered potential" (the regular potential plus an additional one due to randomly distributed defects) for charge carriers similar to the case of the Zn-doped T^* sample may exist in the nonsuperconducting 2:2:3 sample. This is considered to be one of the causes for the dependence of T_c on the L^{3+} ionic radius in the 2:2:3 phase. The lattice distortion inherent to the 2:2:3 phase and the generation of oxygen vacancies in the O(4) or O(2) site, both of which seem to be enhanced as the size of the L^{3+} ion decreases, are possible sources of the disordered potential.

ACKNOWLEDGMENTS

We would like to thank Dr. S. Tajima of Superconductivity Research Laboratory, Dr. N. Nagaosa of University of Tokyo, and N. Fukushima and Dr. S. Tanaka, both of Toshiba R&D Center, for stimulating discussions.

*Present address: Advanced Research Laboratory, Toshiba Research & Development Center, 1, Komukai Toshiba-cho, Saiwai-ku, Kawasaki, 210, Japan.

†Present address: Central Research Laboratories, Matsushita Electric Industrial Co., Ltd. Moriguchi, Osaka 570, Japan.

‡Present address: Electron Microscope Centre, University of Queensland, Brisbane, Queensland, 4072, Australia.

[1]Y. Tokura and T. Arima, Jpn. J. Appl. Phys. **29**, 2388 (1990).

[2]T. Kaneko, H. Yamauchi, and S. Tanaka, Physica C **178**, 377 (1991).

[3]J. B. Torrance, Y. Tokura, A. I. Nazzal, A. Bezinge, T. C. Huang, and S. S. P. Parkin, Phys. Rev. Lett. **61**, 1127 (1988).

[4]Y. Tokura, J. B. Torrance, T. C. Huang, and A. I. Nazzal, Phys. Rev. B **38**, 7156 (1988).

[5]N. P. Ong, in *Physical Properties of the High-Temperature Superconductors II*, edited by D. M. Ginsberg (World Scientific, Singapore, 1990), p. 459.

[6]J. Clayhold, N. P. Ong, Z. Z. Wang, J. M. Tarascon, and P. Barboux, Phys. Rev. B **39**, 7324 (1989).

[7]H. Sawa, K. Obara, J. Akimitsu, Y. Matsui, and S. Horiuchi, J. Phys. Soc. Jpn. **58**, 2252 (1989).

[8]T. Wada, A. Ichinose, Y. Yaegashi, H. Yamauchi, and S. Tanaka, Jpn. J. Appl. Phys. **29**, L266 (1990).

[9]J. M. Tarascon, W. R. McKinnon, L. H. Greene, G. W. Hull, and E. M. Vogel, Phys. Rev. B **36**, 226 (1987).

[10]S-W. Cheong, Z. Fisk, J. D. Thompson, and R. B. Schwarz, Physica C **159**, 407 (1989).

[11]J. T. Markert, J. Beille, J. J. Neumeier, E. A. Early, C. L. Seaman, T. Moran, and M. B. Maple, Phys. Rev. Lett. **64**, 80 (1990).

[12]T. Arima, Y. Tokura, H. Takagi, S. Uchida, R. Beyers, and J. B. Torrance, Physica C **168**, 79 (1990).

[13]T. Maeda, K. Sakuyama, N. Sakai, H. Yamauchi, and S. Tanaka, Physica C **177**, 337 (1991).

[14]S. Ikegawa, T. Wada, A. Ichinose, T. Yamashita, T. Sakurai, Y. Yaegashi, T. Kaneko, M. Kosuge, H. Yamauchi, and S. Tanaka, Phys. Rev. B **41**, 11 673 (1990).

[15]S. Ikegawa, T. Wada, T. Yamashita, A. Ichinose, K. Matsuura, K. Kubo, H. Yamauchi, and S. Tanaka, Phys. Rev. B **43**, 11 508 (1991).

[16]A. Fert and P. M. Levy, Phys. Rev. B **36**, 1907 (1987).

[17]S. Ikegawa, T. Yamashita, T. Sakurai, R. Itti, H. Yamauchi, and S. Tanaka, Phys. Rev. B **43**, 2885 (1991).

[18]K. Kurusu, H. Takami, and K. Shintomi, Analyst **114**, 1341 (1989).

[19]T. Wada, A. Ichinose, Y. Yaegashi, H. Yamauchi, and S. Tanaka, Phys. Rev. B **41**, 1984 (1990).

[20]R. D. Shannon, Acta Crystallogr. A **32**, 751 (1976).

[21]J. H. Van Vleck, *The Theory of Electric and Magnetic Susceptibilities* (Oxford University Press, London, 1932), p. 235.
[22]M. Tovar, D. Rao, J. Barnett, S. B. Oseroff, J. D. Thompson, S-W. Cheong, Z. Fisk, D. C. Vier, and S. Schultz, Phys. Rev. B **39**, 2661 (1989).
[23]C. L. Seaman, N. Y. Ayoub, T. Bjørnholm, E. A. Early, S. Ghamaty, B. W. Lee, J. T. Markert, J. J. Neumeier, P. K. Tsai, and M. B. Maple, Physica C **159**, 391 (1989).
[24]G. H. Kwei, R. B. Von Dreele, S-W. Cheong, Z. Fisk, and J. D. Thompson, Phys. Rev. B **41**, 1889 (1990).
[25]N. Ohashi, H. Ikawa, O. Fukunaga, M. Kobayashi, and J. Tanaka, Physica C **177**, 377 (1991).
[26]M. Kosuge, S. Ikegawa, N. Koshizuka, and S. Tanaka, Physica C **176**, 373 (1991).
[27]M. Kosuge and K. Kurusu, Jpn. J. Appl. Phys. **28**, L810 (1989).
[28]The mixed-valence state of Sm in $SmBa_2Cu_3O_{7-\delta}$ was recently suggested by M. Guillaume, P. Allenspach, J. Mesot, U. Staub, A. Furrer, V. Trunov, A. Kurbakov, H. Blank, and H. Mutka, Physica C **185-189**, 819 (1991).
[29]Such an interaction between the magnetic moment of the Sm ion and charge carrier probably exists in $Sm_{1.5}Ce_{0.15}CuO_{4-\delta}$ in which the temperature dependence of the upper critical field is affected by an antiferromagnetic ordering of Sm ions, as reported by Y. Dalichaouch, B. W. Lee, C. L. Seaman, J. T. Markert, and M. B. Maple, Phys. Rev. Lett. **64**, 599 (1990).
[30]T. Tamegai and Y. Iye, Physica B **165&166**, 1549 (1990); Phys. Rev. B **44**, 10 167 (1991).
[31]T. Tamegai, Y. Iye, M. Ogata, K. Obara, and J. Akimitsu, Jpn. J. Appl. Phys. **28**, L1537 (1989).
[32]F. Izumi, E. Takayama-Muromachi, A. Fujimori, T. Kamiyama, H. Asano, J. Akimitsu, and H. Sawa, Physica C **158**, 440 (1989).
[33]P. Bordet, S-W. Cheong, Z. Fisk, Th. Fournier, J. L. Hodeau, M. Marezio, A. Santoro, and A. Varela, Physica C **171**, 468 (1990); P. Bordet, R. Argoud, C. Chaillout J. Chenavas, S-W. Cheong, Th. Fournier, J. L. Hodeau, M. Marezio, J. Muller, and A. Varela, Physica C **185-189**, 541 (1991).
[34]F. Izumi, H. Kito, H. Sawa, J. Akimitsu, and H. Asano, Physica C **160**, 235 (1989).
[35]For a review, see Patrick A. Lee and T. V. Ramakrishnan, Rev. Mod. Phys. **57**, 287 (1985).
[36]Naoto Nagaosa and Patrick A. Lee, Phys. Rev. Lett. **64**, 2450 (1990).
[37]L. B. Ioffe, V. Kalmeyer, and P. B. Wiegmann, Phys. Rev. B **43**, 1219 (1991).
[38]Naoto Nagaosa and Patrick Lee, Phys. Rev. B **43**, 1233 (1991).
[39]Naoto Nagaosa (private communication).
[40]A. B. Kaiser and C. Uher, in *Studies of High Temperature Superconductors*, edited by A. V. Narlikar (Nova, New York, 1991), Vol. 7, p. 353.
[41]A. B. Kaiser and G. Mountjoy, Phys. Rev. B **43**, 6266 (1991).
[42]M. Suzuki, Phys. Rev. B **39**, 2312 (1989).
[43]B. Fisher, G. Koren, J. Genossar, L. Patlagan, and E. L. Gartstein, Physica C **176**, 75 (1991).
[44]M. Z. Cieplak, G. Xiao, A. Bakhshai, and C. L. Chien, Phys. Rev. B **39**, 4222 (1989).
[45]J. L. Peng, R. N. Shelton, and H. B. Radousky, Phys. Rev. B **41**, 187 (1990).
[46]For a review, see G. Bergmann, Phys. Rep. **107**, 1 (1984).
[47]H. Fukuyama, J. Phys. Soc. Jpn. **49**, 644 (1980).
[48]B. L. Altschuler, D. Khmel'nitzkii, A. I. Larkin, and P. A. Lee, Phys. Rev. B **22**, 5142 (1980).
[49]C. Castellani, C. Di Castro, M. Grilli, and G. Strinati, Phys. Rev. B **37**, 6663 (1988).
[50]F. S. Galasso, *Structure and Properties of Inorganic Solids* (Pergamon, Oxford, 1970), pp. 90–95.
[51]M. Yoshida, S. Tajima, T. Wada, Y. Mizuo, T. Takata, Y. Yaegashi, A. Ichinose, H. Yamaichi, N. Koshizuka, and S. Tanaka, in *Proceedings of the 2nd ISSP International Symposium of Physics and Chemistry of Oxide Superconductors* (PCOS'91), Tokyo, Japan, 1991, edited by H. Yasuoka, H. Fukuyama, and Y. Iye (Springer, Tokyo, in press).
[52]H. Fukuyama, Physica B **126**, 306 (1984); S. Maekawa and H. Fukuyama, J. Phys. Soc. Jpn. **51**, 1380 (1981).